

Evaluation of Biogenic Silver Nanoparticles Synthesized from Vegetable Waste

Bushra Hafeez Kiani¹, Irshad Arshad², Sodha Najeeb¹, Mohammed K Okla³, Taghreed N Almanaa³, Wahidah H Al-Qahtani⁴, Mostafa A Abdel-Maksoud³

¹Department of Biological Sciences (Female Campus), Faculty of Basic and Applied Sciences, International Islamic University, Islamabad, Pakistan; ²Department of Biology, New Mexico Highland University, Las Vegas, NM, USA; ³Botany and Microbiology Department, College of Science, King Saud University, Riyadh, Saudi Arabia; ⁴Department of Food Sciences & Nutrition, College of Food and Agricultural Sciences, King Saud University, Riyadh, Saudi Arabia

Correspondence: Bushra Hafeez Kiani, Department of Biological Sciences (Female Campus), Faculty of Basic and Applied Sciences, International Islamic University, Islamabad, 44000, Pakistan, Email bushra.hafeez@iiu.edu.pk; Mostafa A Abdel-Maksoud, Botany and Microbiology Department, College of Science, King Saud University, Riyadh, 2455, Saudi Arabia, Email mabdmaksoud@ksu.edu.sa

Introduction: Vegetable waste has numerous essential values and can be used for various purposes. Unfortunately, it is often discarded worldwide due to a lack of awareness regarding its nutritional and practical significance. Even the nutrient-rich peels of fruits and vegetables are commonly wasted, despite their numerous useful applications. Utilizing vegetable waste to produce silver nanoparticles through green synthesis is an advantageous, economical, and environmentally friendly method for producing valuable products while addressing waste management concerns. The main emphasis of this study was to synthesize silver nanoparticles (AgNPs) by using vegetable waste from *Solanum tuberosum* (potato) and *Coriander sativum* (coriander).

Methods: The stems of *Coriander sativum* and peels of *Solanum tuberosum* were used as extracts for the synthesis of AgNPs. The characterization of the synthesized AgNPs involved UV-spectroscopy, scanning electron microscopy (SEM), and X-ray diffraction (XRD). The phytochemical analysis was performed to analyze antimicrobial, cytotoxic, antidiabetic, antitumor, antioxidant, alpha-amylase, and protein inhibition activities.

Results: The change in the color of the reaction mixture from yellowish green to brown following the addition of extracts to the silver nitrate solution confirmed nanoparticle synthesis. UV analysis has shown peaks in the range of 300–400nm. SEM confirmed the spherical and agglomerated morphology and size of 64nm for potato peel and 70nm for coriander stem. XRD confirmed the crystalline structure of silver nanoparticles. The phytochemical assays confirmed that silver nanoparticles had higher total phenolic and flavonoid contents. The biosynthesized silver nanoparticles showed promising antimicrobial, cytotoxic, antidiabetic, antitumor, and antioxidant properties and significant alpha-amylase and protein inhibition activities in comparison with the crude extracts.

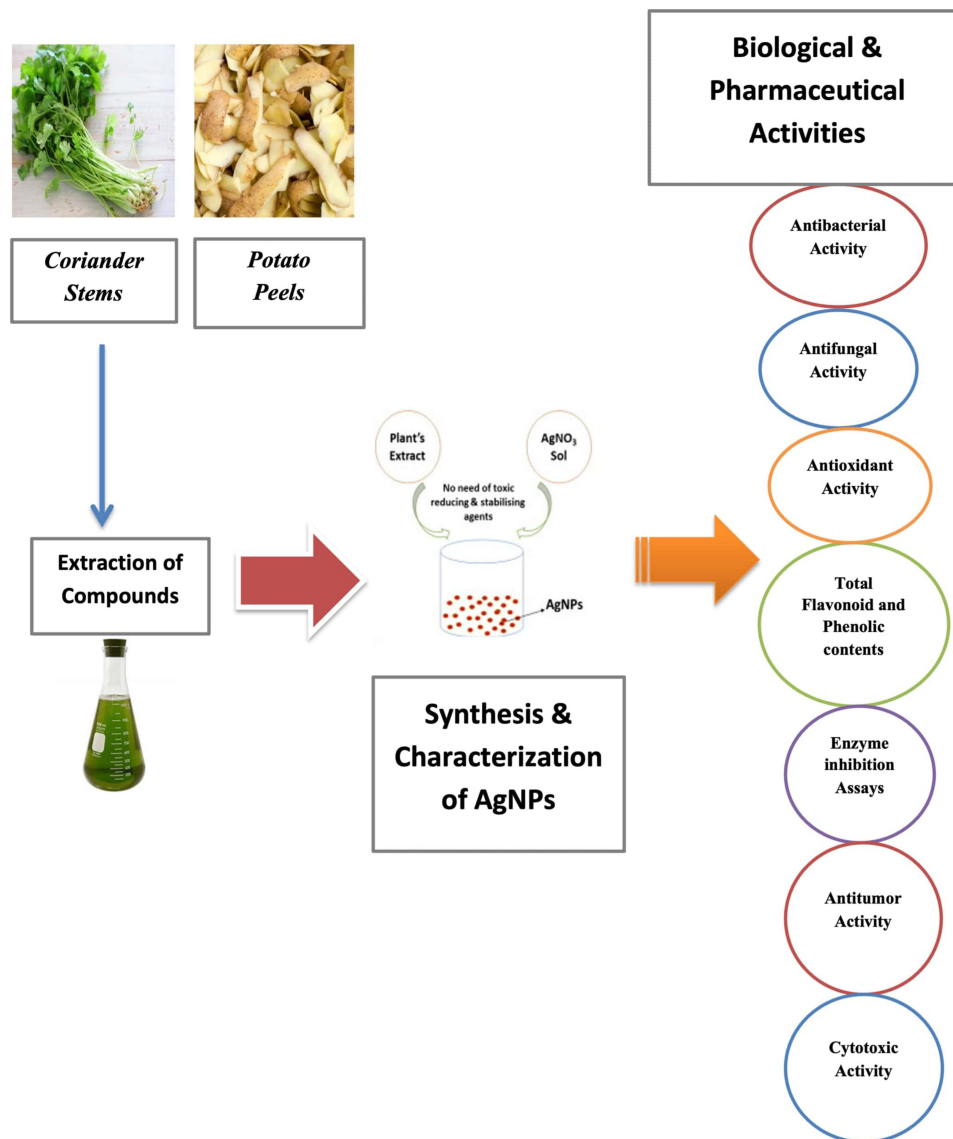
Conclusion: The bioactivity of the plant suggests that it could be a suitable option for therapeutic purposes. This study demonstrates a potential method for sustainable nanoparticle synthesis and the therapeutic applications of AgNPs derived from vegetable waste. By utilizing the potential of vegetable waste, we can contribute to both environmental sustainability and the development of innovative, valuable products in fields such as medicine, agriculture, and materials science. These findings encourage further research on agricultural byproducts, promoting environmentally friendly and economically advantageous research and development efforts.

Keywords: silver nanoparticles, vegetable waste, antimicrobial, antidiabetic, *Coriander sativum*, *Solanum tuberosum*

Introduction

The field of nanotechnology is rapidly emerging and gaining worldwide popularity, primarily driven by the unique physical and biochemical characteristics exhibited by nanomaterials. It significantly improves techniques to produce new products of controlled size and shape at the nanometer scale.¹ Nanoparticles display a significant role for living organisms, playing an excellent role in the field of medicine, energy production, and storage. Several methods are available to synthesize metal nanoparticles, including chemical, green, physical, and hybrid methods.² Normally,

Graphical Abstract



chemical and physical methods are not eco-friendly; they are toxic and yield low. The isolation and preparation of culture media for microorganisms for the synthesis of nanoparticles is costly.

Plants are alternatively providing a better platform for the cost-effective synthesis of nanoparticles.³ Furthermore, they are biocompatible and environmentally friendly. There are several starting materials for the green synthesis of nanoparticles, including plants, fruits,⁴ roots, and calluses. Vegetable waste has numerous essential values and can be used for different purposes. However, it is mostly discarded by people worldwide because people often do not know the essential values of this waste. Advantageous vegetable waste includes peels of fruits and vegetables, which are rich in many nutrients and vitamins and are also discarded despite their many important uses. For example, peels of apples contain essential minerals and vitamins, including vitamin A, vitamin K, vitamin C, and much calcium and potassium, phenolic compounds, dietary fiber, and have strong antioxidant activity.⁵ Banana peels are nowadays used to treat skin problems like irritations, allergies, acne, dark spots, and wrinkles in homemade remedies due to their strong antioxidant

properties.⁶ Stems of different vegetables, eg, coriander, are rich in nutrients having antimicrobial activities. Peels of potatoes are rich in dietary fiber, and a natural antioxidant is also discarded as a byproduct.⁷

Metallic and metal oxide nanoparticles find multiple applications across various industries and disciplines, including agriculture, catalyst development, bio-labelling, and biomedical sciences. Due to the distinct qualities of silver nanoparticles, they are extensively used in chemical sensing, photonics, pharmaceuticals, biosensing, electronics, and catalysis.⁸ Silver nanoparticles are added to containers for food storage, home appliances, and medical instruments to avoid contamination due to their antimicrobial properties.⁹ In addition to antimicrobial activities, they also exhibit antitumor and antiplatelet properties.¹⁰ Using vegetable waste to synthesize silver nanoparticles represents a distinctive concept within green synthesis. The benefits of this approach are the utilization and management of waste and the synthesis of silver nanoparticles in a natural environment at a low cost and nontoxic way. They can also be easily and rapidly resynthesized.

Due to the vast biological potential of vegetable waste, the current research used vegetable waste (potato peels and coriander stems) to synthesize the silver nanoparticles. The primary focus of the current study was to assess the medicinal properties of silver nanoparticles, including their cytotoxic, anti-bacterial, and anti-cancer activities, as well as their antioxidative characteristics. In addition, the level of secondary metabolites (flavonoids, alkaloids, phenolics) were also compared between AgNPs and crude extracts. The present study also conducted experiments on enzyme inhibition specifically, protein kinase and alpha-amylase inhibition to assess the efficacy of silver nanoparticles (AgNPs) against enzymatic proteins.

Materials and Methods

Collection of Plant Samples

The plant samples (potato peels and coriander stems) were collected from the kitchen vegetable waste. These plants were identified by Prof. Dr. Rizwana Aleem Qureshi (Taxonomist), Department of Plant Sciences, Quaid-i-Azam University, Islamabad. A voucher specimen number [HMP-731 (potato peels) and HMP-732 (coriander stems)] was deposited in the public herbarium ie The National Herbarium of Pakistan, Islamabad, Pakistan. The samples were carefully separated, cleaned to remove any dirt or impurities, and then allowed to dry in a shaded area. Subsequently, the dehydrated peels and stems were ground using a mortar and pestle to obtain a powdered sample, which was stored separately for future use.

Plant Extraction

The dried parts of potato peels and coriander stems were used to prepare extracts by using distilled water as a solvent. First, 60 g of the plant powder of potato (*Solanum tuberosum*) peels and coriander stems (*Coriandrum sativum*) was soaked in 100mL of distilled water and left at room temperature (23–27°C) for three days.

To extract the compounds, ultra-sonication was used in an ultrasonic bath for a duration of 30 minutes at a temperature range of 23–27°C. The obtained extracts were subjected to filtration using Whatman filter No. 1 paper. The filtration process was repeated twice, and all the extracts were combined to obtain the final concentration of the extracts for further processing. The combined extracts were concentrated through evaporation using a vacuum rotary evaporator. Lastly, the concentrated extracts were subjected to drying in a vacuum dryer set at 45°C for the final crude extracts.

Synthesis of Silver Nanoparticles

AgNPs were synthesized by combining 10 mL of the potato peels and coriander stem extracts with a 1 mM silver nitrate solution (AgNO₃). The mixtures were incubated in the dark for 24 hours to avoid silver nitrate photochemical activation. After 24 hours, a noticeable color change was observed, indicating the successful synthesis of AgNPs. The extract was finely spread in the form of a thin layer onto Petri plates and dried at 60°C overnight in a drying oven. Once fully dried, the resulting powder is used for the subsequent characterization process. The same process was repeated for all the extracts.

Characterization of Zinc Oxide Nanoparticles

UV-Visible Spectroscopy

UV-Vis spectroscopy is a commonly used technique for nanoparticle characterization, as described by.¹¹ This method follows the principles of the Beer-Lambert law, as mentioned by.¹² In the case of silver nanoparticles, their characterization was performed using a wavelength range of 300–400 nanometers. A spectroscope was used to examine the material, and the spectra were monitored within the range of 300 to 700 nanometers with a resolution of 1 nanometer.

Scanning Electron Microscopy Analysis (SEM)

Scanning electron microscopy (KYKY-EM6900) was used to analyze the size and shape of the AgNPs, as outlined in the study by.¹³ A droplet of the AgNPs sample solution was placed onto a grid coated with carbon to evaluate the silver nanoparticles, ensuring an even distribution of the nanoparticles. The sample was then dehydrated for 15 minutes using a mercury lamp at 30 kV and the results were photographed using the SEM.

X-Ray Diffraction (XRD)

The crystal structure of the AgNPs was analyzed by X-ray diffraction (XRD) using a Cu K α radiation source ($\lambda = 1.540562 \text{ \AA}$). The XRD analysis was performed for a duration of 2 hours at 30–40 kV and 15 mA. The measurements were taken on a 20-degree scale with a step size of 0.02 degrees.

Phytochemical Analysis

Total Flavonoid Content

To analyze the complete flavonoid concentration, we followed the methodology described by.¹⁴ Initially, 20 μL of extracts were mixed with 10 μL of potassium acetate, 10 μL of aluminium chloride, and 160 μL of distilled water in 96-well plates. The mixture was then incubated at room temperature for 30 minutes. Absorbance readings were taken at a wavelength of 405 nanometers using a microplate reader. To determine the total flavonoid concentrations in terms of quercetin equivalence, a standard curve was established using quercetin solutions ranging from 2.5 to 40 $\mu\text{g/mL}$. As a negative control, 20 μL of the respective solvents were utilized in the analysis.

Total Phenolic Concentration Assessment

The Folin–Ciocalteu reagent method was employed to assess the complete phenolic content, following the procedure described by.¹⁴ Extract solutions were prepared at a concentration of 1mg/ μL . A volume of 200 μL of the extract solution was combined with 90 μL of Folin–Ciocalteu in a 96-well plate. The entire mixture was incubated at room temperature for 5 minutes. Subsequently, 90 μL of sodium carbonate was added, and the mixture was incubated again for 60 minutes at room temperature. The phenolic content was measured at a wavelength of 630 nm using a microplate reader. Gallic acid solutions ranging from 3.125 to 25 $\mu\text{g/mL}$ were utilized to establish a standard calibration curve. The total phenolic content was expressed as a percentage weight by weight in gallic acid equivalents. As a negative control, 20 μL of the respective solvents were used in the analysis.

Biological Activities

The following biological activities of silver nanoparticles from vegetable waste were performed.

Antibacterial Assay

The disc diffusion method was used according to the methodology of¹⁵ for the analysis of the antibacterial properties of the extracts. The antibiotic activity was tested against five bacterial strains, including *Staphylococcus aureus* (ATCC 6538) and *Bacillus subtilis* (ATCC 6633) as monograms, and *Pseudomonas aeruginosa* (ATCC-15442), *Escherichia coli* (ATCC 15224), and *Klebsiella pneumoniae* (ATCC-1705) as sidearms. A bacterial lawn was prepared on nutrient agar plates by streaking a fresh culture of each bacterial strain at a seeding density of 1×10^6 CFU/mL. Sterile filter paper discs were impregnated with each test extract (5 μL from a 20 mg/mL DMSO solution). Positive controls included Cefixime and roxithromycin (5 μL from a 4 mg/mL DMSO solution), while the negative control consisted of DMSO (5 μL). Following 24 hours of incubation at 37°C, the discs were carefully placed onto agar plates labelled accordingly

with the corresponding bacteria. The resulting inhibition zones around each disc were measured. This test was repeated thrice, and the mean value and standard deviation were determined.

To determine the Minimum Inhibitory Concentration (MIC), the technique described by¹⁵ was followed. Samples displaying notable inhibition zones (ie, ≥ 12 mm) were further analyzed using the micro broth dilution technique. Bacterial inoculum densities were adjusted to a predetermined 5×10^4 CFU/mL density. To conduct the micro broth dilution technique, three-fold serial dilutions of each experimental sample were prepared in nutrient broth. The bacterial cultures were incubated in the broth for 11 hours and refrigerated at 4°C.

Antifungal Assay

The antifungal activity was analyzed against various fungal strains, including *Aspergillus fumigatus* (FFBP 66), *Mucor* species (FFBP 0300), *Fusarium solani* (FFBP 0291), and *Aspergillus flavus* (FFBP 0064) by following the methodology of.¹⁵ The fungal strains were cultured on Sabouraud dextrose agar (SDA) plates at a temperature of 28°C and a pH level of 5.7. The fungal cultures were stored in a refrigerator at 4°C for future use. Clotrimazole (4 mg/mL) was utilized as the standard treatment and DMSO was used as a negative control. SDA plates were inoculated with 100 μ L of the fresh fungal inoculum and filter paper discs with the test extracts (5 μ L, 20 mg/mL DMSO), DMSO (5 μ L), and clotrimazole (5 μ L, 4 mg/mL DMSO) were spread on the seeded SDA plates. The inoculated plates were incubated at 30°C for 24 hours and inhibition zones were measured to assess the antifungal activity.

Brine Shrimp Cytotoxicity Assay

The brine shrimps' eggs were spawned in a rectangular pan measuring 22 \times 32 cm, filled with salt water, and brine shrimp (*Artemia salina*) eggs. A plastic separator with several holes measuring 2mm in thickness was placed inside the pan to create two distinct sections. One section of the experiment was shaded with aluminium foil to create different lighting conditions, while the other section was left exposed to light. The brine shrimp eggs (approximately 25mg) were dispersed in the larger shaded section, while the separator prevented them from reaching the lighted section. Following a day of hatching, the phototropic nauplii (brine shrimp larvae) were collected from the illuminated section using a pipette. The larvae were collected once they had separated from their eggshells through the holes in the separator.

For the cytotoxicity experiment, a 96-well plate was utilized, with wells labelled alphabetically from A to H. Wells A and E were filled with 44 μ L of seawater, while wells B, C, D, F, G, and H received 25 μ L of seawater. Wells A and E received 6 μ L of the sample being tested. From well A, 25 μ L of the sample was transferred to well B, and the process was repeated from B to C. The same procedure was followed for wells D, E, F, G, and H, except that 25 μ L of the sample was discarded from well D. This process ensured uniform dilution values across the plate. Ten brine shrimp larvae were carefully transferred into each microplate well, and the remaining volume was supplemented with 300 μ L of seawater across all wells. The microplate was then incubated for 24 hours. The survival of the larvae was observed using a microscope, and the experiment was repeated three times to ensure reliability. The percentages of deceased larvae in each well were calculated using Abbott's method.

Antitumor Assay

The antitumor potato disc assay was carried out following the below procedure. A 48-hour-old culture of the *Agrobacterium tumefaciens* strain was used as a testing medium for the plant extracts. Inoculum was prepared by combining 1.5 mL of bacterial cultures, distilled water, and three different concentrations of plant extracts (1000, 500, and 100 μ g/mL). DMSO was used as the negative control, while vinblastine sulfate was used as the positive control. To begin, red-skinned potatoes were surface sterilized with a 0.1% HgCl₂ solution and then washed three times with distilled water. Potato cylinders were obtained using an 8 mm diameter borer and sliced into 4 mm discs. Petri dishes (20 mL) were filled with agar solution (1.5% w/v) and allowed to solidify. In each Petri dish, ten potato discs were meticulously arranged on the agar surface, and 50 μ L of the prepared inoculum was poured onto each disc. The plates were sealed with parafilm to preserve moisture and then incubated in the dark at a temperature of 28°C. Following a 21-day incubation period, the potato discs were stained with Lugol's solution (10% KI, 5% I₂), and the number of tumors was counted under a dissecting microscope. Any tumor inhibition exceeding 20% was regarded as significant. The tumor inhibition percentage was calculated using the following formula:

$$\% \text{ of tumor inhibition} = ((1 - T_s)/T_c) \times 100$$

Where “Ts” represents the number of tumors in the sample and “Tc” represents the number of tumors in the control.

Analysis of Cytotoxic Activity on HEp-2 Cell Lines

The MTT assay was performed to evaluate the cytotoxic activity of AgNPs synthesized from vegetable waste extracts and was also analyzed on HEp-2 cell lines (provided by institute of Biomedical and Genetic Engineering (IBGE), Islamabad). The HEp-2 cell lines with 10% of FCS and cancer-containing cells were sown in Minimal media and incubated at 37°C in the presence of 5% carbon dioxide. The cells were trypsinized for 3–5, and after 24h incubation, they were centrifuged for 5 minutes at 1400 rpm. The ELISA cells were distributed in 96 well plates, and in every plate, 300,000 cells were placed and incubated for 24h at 37°C degree in the presence of 5% carbon dioxide.¹⁶

Free Radical Scavenging Activity

The free radical scavenging activity of the extracts was assessed using the DPPH (2, 2-diphenyl-1-picrylhydrazyl) assay, following the methodology described by.¹⁷ To begin, 9.6 mg of DPPH was dissolved in 100 mL of methanol to form a DPPH solution. The tested samples were prepared in Dimethyl sulfoxide (DMSO) at a concentration of 4 mg/mL, while ascorbic acid was used as a positive control at a concentration of 1 mg/mL. DMSO served as the negative control standard. In a 96-well plate, each well received 10 µL of the test substance, followed by 190 µL of the DPPH reagent. The mixture was exposed to light for one hour at 37°C, and the absorbance was measured at 515nm. The experiment was repeated three times, and the IC50 values were calculated using table curve software. The % inhibition was computed using the following equation:

$$\% \text{ DPPH} = (1 - \text{Abs}/\text{Abc}) \times 100$$

Where “Abs” represents the absorbance of the experimental sample and “Abc” represents the absorbance of the negative control.

Enzyme Inhibition Assays

Protein Kinase Assay

As per the procedures by,¹⁸ the hyphae production of pure strain *Streptomyces* 85E was examined in this experiment. The sterile plates with minimal ISP4 media were prepared, and spores (mycelia fragments) from a fresh *Streptomyces* culture were evenly dispersed to form a bacterial lawn. Next, extracts were applied to sterilized 6mm filter paper discs at a volume of 5 µL (20 mg/mL in dimethyl sulfoxide). These impregnated paper discs, each containing 100 micrograms of bacteria, were placed on the plates of *Streptomyces* 85E and incubated for three days at 30°C. To assess the inhibitory effects, negative controls using dimethyl sulfoxide and positive controls with Surfactin-containing discs were used. The evaluation of the results involved analyzing the presence of a distinct inhibitory zone around the discs containing the various samples and controls.

α-Amylase Inhibition Assay

The anti-diabetic potential of the sample extracts was evaluated using a modified version of the α-amylase inhibition assay described by.¹⁹ In this assay, a reaction mixture containing amylase, phosphate buffer, starch solution, and the sample extracts was prepared in a 96-well plate. The amylase concentration used was 0.14 U/mL, while the sample extracts were added at 4mg/mL in Dimethyl sulfoxide. The mixture was then incubated at 50 °C for 30 minutes. This assay allows for assessing the inhibitory activity of the sample extracts against α-amylase, an enzyme involved in the breakdown of carbohydrates. The enzymatic reaction was halted by adding 20 µL of a 1 molar hydrochloric acid solution. Afterwards, each well was filled with 90 µL of an iodine solution consisting of 5 mM iodine and 5 mM potassium iodide. The negative control consisted of samples without any plant extracts. In contrast, the blank samples were prepared without the presence of amylase and plant extract, with the buffer used as a substitute. As a positive control, acarbose at a concentration of 250 µM was utilized. After the incubation period, the absorbance was measured at a wavelength of 540 nm. The α-amylase inhibition activity was quantified as the percentage of inhibition per mg of dry extract. This was determined using the following formula:

$$\% \alpha - \text{amylase inhibition} = [(Ab - As)/Ab] \times 100$$

Where “Ab” represents the absorbance of the blank, and “As” represents the absorbance of the sample.

Statistical Analysis

The experiments were conducted three times to ensure reliability, and the results were presented as the average value along with the standard deviation (SD) to indicate the level of variability. To determine the significance of the observed differences, a statistical analysis known as the least significant difference (LSD) was performed at a significance level of $P \leq 0.05$. This analysis involved comparing the mean values obtained from the different treatments after analyzing variance (ANOVA).

Results

Synthesis of Zinc Oxide Nanoparticles

Silver nanoparticles (AgNPs) were successfully synthesized using distilled water extracts of potato peels and coriander stems. The synthesis process involved treating the extracts with a 1mM AgNO₃ solution while stirring continuously. After 24 hours of incubation, a noticeable change in color occurred, with the solution transforming from light yellow to brown, indicating the synthesis of silver nanoparticles. The solution was then subjected to overnight oven-drying at 60°C, resulting in the formation of a pellet containing pure nanoparticles.

Characterization of Silver Nanoparticles

The silver nanoparticles were subjected to analysis using various techniques, including ultraviolet-visible spectroscopy, scanning electron microscopy (SEM), and X-ray diffraction (XRD). These techniques were utilized to examine and characterize the properties of the synthesized silver nanoparticles.

Ultraviolet-Visible Spectroscopy

Peaks in the 300 to 400 nm range were detected, indicating the presence of silver nanoparticles that were synthesized using the extract derived from vegetable waste (Figure 1A and B).

Scanning Electron Microscopy (SEM)

The scanning electron microscopy (SEM) analysis confirmed that the size of the particles in both extracts was within the range of 100 nm. This finding further proves the successful synthesis of silver nanoparticles using vegetable waste

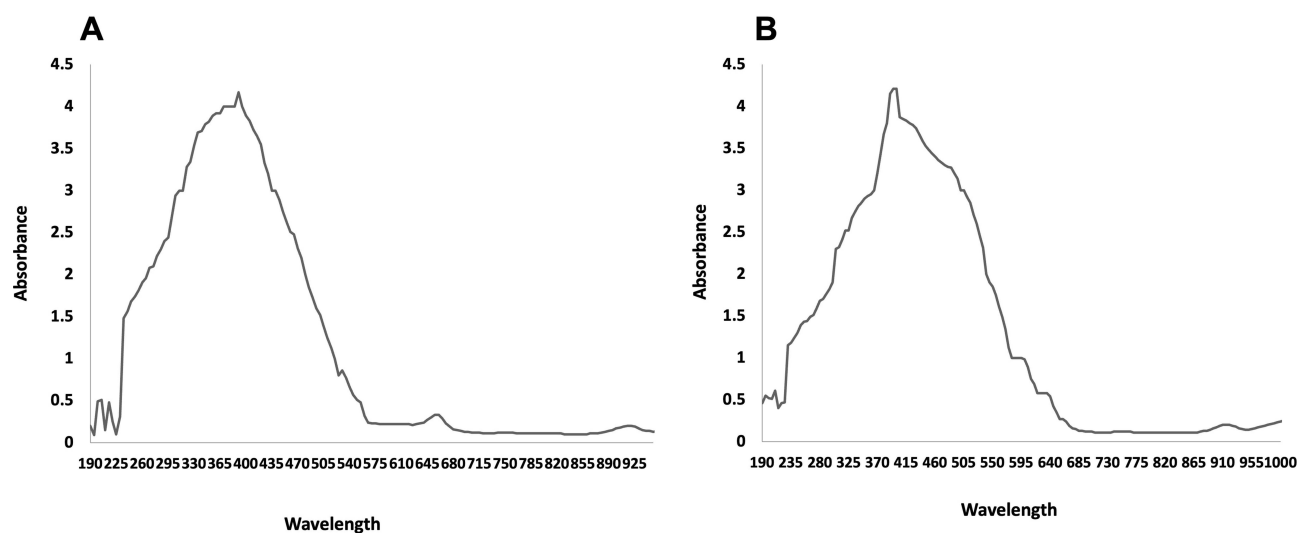


Figure 1 UV visible absorption spectra of silver nanoparticles. (A) Potato peel extracts; (B) coriander stem extract.

extracts. The size was within the 70–90 nm range at 30KV for the synthesized AgNPs. The size of AgNPs was about 65nm for potato peels and 70nm for coriander stem extracts, respectively (Figure 2A and B). The SEM analysis revealed that the shapes of the silver nanoparticles synthesized from the vegetable waste extracts varied, with the predominant spherical shapes. The nanoparticles were observed to be agglomerated, forming clusters. Overall, the SEM analysis demonstrated a well-scattered combination of particles, indicating the presence of synthesized silver nanoparticles with diverse shapes and agglomeration.

X-Ray Diffraction (XRD)

The X-ray diffraction (XRD) pattern analysis confirmed the structural properties of the nanoparticles. The XRD analysis revealed broad halo peaks at 20, 25, 30, 35, and 40 degrees, corresponding to the crystallographic planes of 121, 200, 210, 220, and 311, respectively. These peak patterns indicate the crystalline nature of the silver nanoparticles synthesized by reducing Ag⁺ ions. The XRD results provide evidence of the crystalline structure of the synthesized silver nanoparticles (Figure 3A and B).

Phytochemical Analysis

Total Phenolic Contents

The measured total phenolic content (TPC) of potato peels indicated higher values in the AgNPs (59 ± 0.10) compared to the crude extracts (24.4163 ± 0.18). This suggests that the synthesis of silver nanoparticles enhances the phenolic content present in the potato peel extracts. The higher TPC in the AgNPs indicates a potential increase in the antioxidant and bioactive properties of the synthesized nanoparticles. For coriander stem nanoparticles also showed high values (54.64758 ± 0.21) as compared to control extracts (21.92952 ± 0.37) (Figure 4).

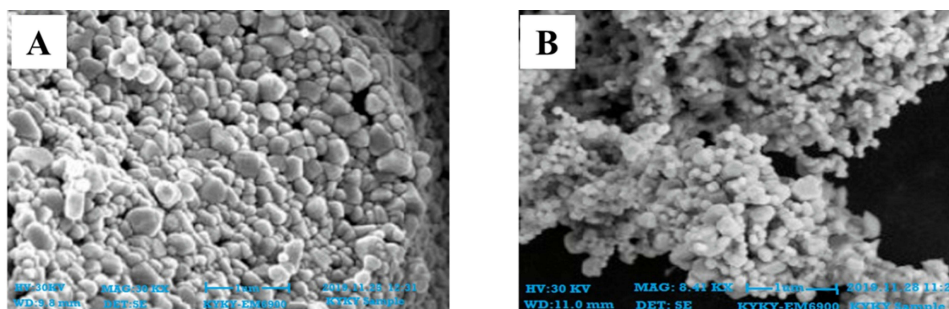


Figure 2 SEM images of silver nanoparticles. (A) Potato peel extracts; (B) coriander stem extract.

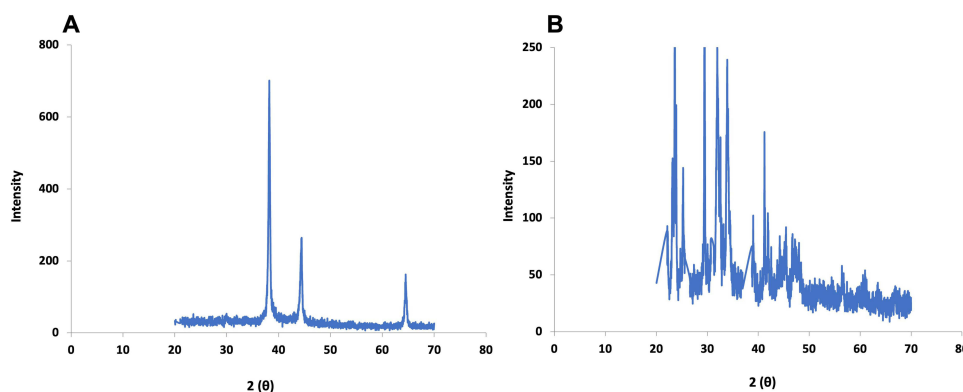


Figure 3 XRD analysis silver nanoparticles. (A) Potato peel extracts; (B) coriander stem extract.

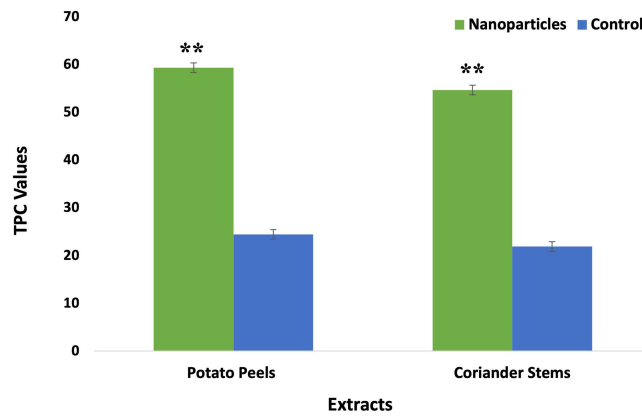


Figure 4 Total phenolic contents of nanoparticles and control extracts. Data are expressed as the mean \pm SD. ** $p < 0.01$.

Total Flavonoid Contents

The highest total flavonoid content (TFC) values were observed in the potato peel nanoparticles (113.01 ± 0.16) compared to the control value (12.745 ± 0.07). Similarly, the coriander stem nanoparticles exhibited higher TFC values (97.48 ± 0.04) than the control (20.564 ± 0.19) (Figure 5). These findings indicate that the synthesis of silver nanoparticles enhances the flavonoid content in potato peel and coriander stem extracts. The increased TFC in the nanoparticles suggests a potential increase in their antioxidant and bioactive properties.

Biological Activities

Antioxidant Assay

The silver nanoparticles (AgNPs) synthesized from potato peel extracts showed strong scavenging activity with an IC_{50} value of $29.26 \mu\text{g/mL}$ at the concentration of $100 \mu\text{g/mL}$, significantly lower than the IC_{50} value of the control extract at $159.46 \mu\text{g/mL}$. Similarly, the AgNPs derived from coriander stem extracts exhibited antioxidant activity with an IC_{50} value of $49.44 \mu\text{g/mL}$ at the concentration of $500 \mu\text{g/mL}$, notably lower than the IC_{50} value of the control extracts at $231.22 \mu\text{g/mL}$ (Figure 6). These results suggest that the synthesis of AgNPs enhances the antioxidant potential of the extracts, making them more effective in scavenging free radicals.

Antibacterial Assay

The antibacterial properties of the potato peel and coriander stem extracts were assessed against various bacterial strains. Extracts that displayed a zone of inhibition equal to or greater than 12 mm were further examined to determine the

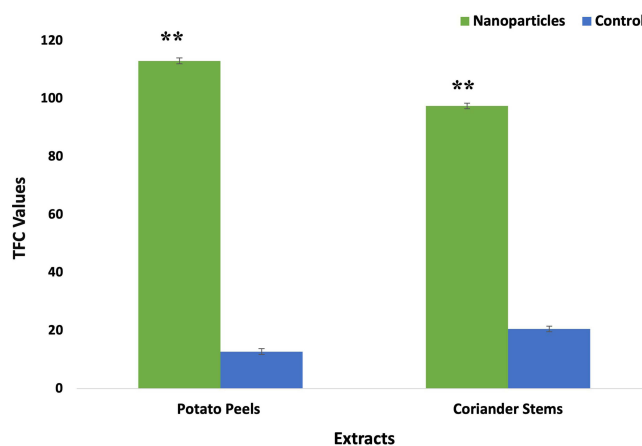


Figure 5 Total flavonoid contents of nanoparticles and control extracts. Data are expressed as the mean \pm SD. ** $p < 0.01$.

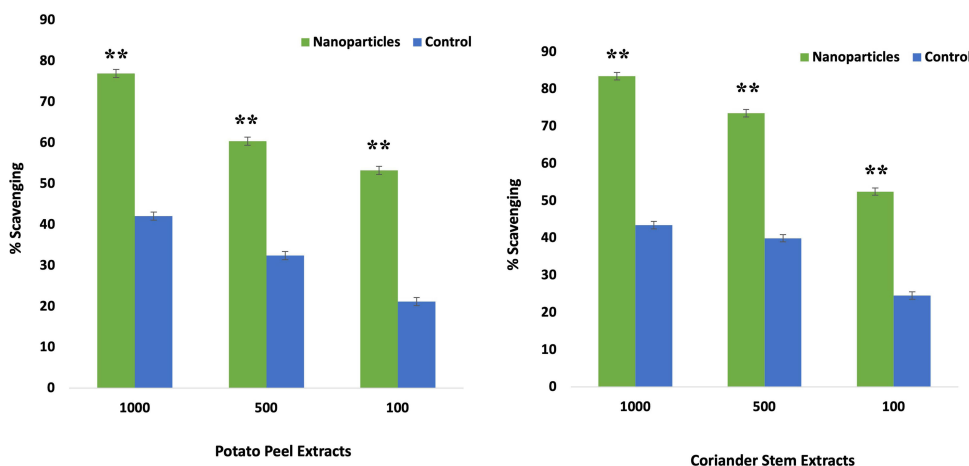


Figure 6 Comparative analysis of antioxidant activity of AgNPs and crude extracts. Data are expressed as the mean ± SD. **p< 0.01.

Minimum Inhibitory Concentration (MIC). In this study, the silver nanoparticles (AgNPs) synthesized from potato peel extracts exhibited the highest antibacterial activity against *E. coli*, with a zone of inhibition measuring 22±0.54 mm at 5 mg/20 mL (MIC 34.3 µg/mL). They also demonstrated significant activity against *B. subtilis*, with a zone of inhibition measuring 18±0.5 mm at the same concentration (MIC 100 µg/mL) (Table 1).

Table 1 Antibacterial Activity and MIC Values of Potato Peels, Coriander Stem and AgNPs

Extracts (mg/mL)	Diameter of Zone of Inhibition in mm (Mean ± SD)* (MIC: µg/mL)										
	Samples	S. A	MIC	B. S	MIC	P. A	MIC	K. P	MIC	E. C	MIC
Potato peels											
5mg/20mL	AgNPs	13±0.45	33.3	9±0.21	–	14±0.76	100	20±0.76	100	22±0.54	34.3
	C	5±0.15	–	7±0.7	–	5±0.15	–	7±0.50	–	8±0.15	–
10mg/20mL	AgNPs	16±0.36	–	13±0.31	33.3	8±0.21	–	16±0.96	100	16±0.31	100
	C	10±0.17	–	8±0.5	–	5±0.15	–	12±0.58	33.3	10±0.58	–
15mg/20mL	AgNPs	16±0.31	100	18±0.5	100	11±0.25	–	15±0.61	100	19±0.50	63.1
	C	9±0.32	–	11±0.3	–	7±0.33	–	12±0.29	33.3	16 ± 0.50	100
Coriander Stems											
5mg/20mL	AgNPs	9±0.9	–	9±0.5	100	7±0.31	–	7±0.55	–	10±0.41	–
	C	9±0.28	–	3±0.3	–	5±0.13	–	6±0.87	–	6±0.51	–
10mg/20mL	AgNPs	20±0.71	41.7	12±0.5	–	9±0.34	–	18±0.61	100	20±0.86	57.4
	C	9±0.36	–	10±0.8	100	7±0.10	–	9±0.76	–	13±0.50	100
15mg/20mL	AgNPs	13±0.12	100	9±0.5	3.7	6±0.55	–	21±0.3	61.3	14±0.5	3.7
	C	10±0.31	–	6±0.5	–	6±0.31	–	7±0.35	–	9±0.50	–
Rox		23±0.54	1.11	17±0.3	3.33	–	–	–	–	–	–
Cefix		–	–	–	–	22±0.89	1.11	20±1.2	1.11	20±1.5	3.33
DMSO		–	–	–	–	–	–	–	–	–	–

Notes: *The sample concentration was 100µg per disc. Values (mean ± SD) are the average of the triplicate analysis of each plant extract (n value of 1×3). – = No activity. Samples showing a zone of inhibition ≥12 mm are not applicable for MIC determination.

Abbreviations: S. A, *Staphylococcus aureus*; B. S, *Bacillus subtilis*; P. A, *Pseudomonas aeruginos*; K. P, *Klebsiella pneumoniae*; E. C, *Escherichia coli*.

Similarly, the AgNPs derived from coriander stem extracts showed significant inhibition against *K. pneumoniae*, with zones of inhibition measuring 20 ± 0.91 mm (MIC 57.4 $\mu\text{g/mL}$) and 18 ± 0.61 mm (MIC 100 $\mu\text{g/mL}$) at a concentration of 10mg/20mL. They also demonstrated notable activity against *S. aureus* and *E. coli*, with zones of inhibition measuring 20 ± 0.71 mm (MIC 41.7 $\mu\text{g/mL}$) and 21 ± 0.3 mm (MIC 63.2 $\mu\text{g/mL}$) at the same concentration (Table 1).

Antifungal Assay

The antifungal activity of the experimental extracts was evaluated against fungal strains using the disc diffusion method. Both extracts, especially nanoparticles, exhibited significant antifungal activity compared to the control extracts. The silver nanoparticles (AgNPs) derived from potato peel extracts displayed the highest antifungal activity against *A. flavus*, with a zone of inhibition measuring 15 ± 0.2 mm at a concentration of 10 mg/20 mL (MIC 24.3 $\mu\text{g/mL}$) when compared to other fungal strains (Table 2).

In the case of coriander stem, AgNPs extracts showed significant antifungal activity against *F. solani* ie, 19 ± 0.31 mm (MIC 13.7 $\mu\text{g/mL}$), compared to other fungal strains at the concentration of 10 mg/20 mL (Table 2).

Cytotoxicity Activity

The cytotoxicity of the test samples was assessed by measuring their impact on *Artemia salina* nauplii. The extracts derived from silver nanoparticles (AgNPs) showed significant toxicity, resulting in a high mortality rate among the nauplii. AgNPs synthesized from potato peel extract displayed substantial cytotoxic activity ie $88 \pm 0.11\%$ with an LC_{50} (lethal concentration that causes 50% mortality) value of 24.83 $\mu\text{g/mL}$ as compared to control extracts ie, $51 \pm 0.49\%$ with LC_{50} value of 89.66 $\mu\text{g/mL}$ (Figure 7).

Table 2 Antifungal Activity and MIC Values of Potato Peels, Coriander Stem and AgNPs

Extracts (mg/mL)	Samples	<i>A. flavus</i>	MIC	<i>A. fumigatus</i>	MIC	<i>Mucor sp.</i>	MIC	<i>F. solani</i>	MIC
Potato peels									
5mg/20mL	AgNPs	9±0.25	43.3	12±0.12	–	11±0.67	100	11±0.76	–
	C	6±0.13	–	8±0.3	–	6±0.15	100	8±0.50	–
10mg/20mL	AgNPs	15±0.2	24.3	11±0.14	31.3	7±0.12	–	11±0.96	100
	C	9±0.13	–	7±0.4	–	5±0.15	100	13±0.85	100
15mg/20mL	AgNPs	11±0.13	100	13±0.4	100	11±0.25	–	11±0.16	100
	C	8±0.23	–	10±0.3	–	7±0.33	–	6±0.92	–
Coriander Stems									
5mg/20mL	AgNPs	10±0.7	–	11±0.3	100	8±0.13	–	7±0.34	100
	C	6±0.82	100	5±0.5	–	6±0.65	–	4±0.78	–
10mg/20mL	AgNPs	11±0.51	100	13±0.3	–	8±0.11	–	19±0.31	13.7
	C	5±0.63	–	7±0.17	100	7±0.13	–	7±0.49	–
15mg/20mL	AgNPs	10±0.21	100	10±0.34	100	8±0.87	–	11±0.18	100
	C	7±0.13	–	6±0.37	–	3±0.83	–	4±0.35	–
Controls									
Clotrim		22±0.89	1.11	20±1.2	1.11	20±1.5	1.11	21±0.6	1.11
DMSO	–	–	–	–	–	–	–	–	–

Notes: Mean \pm SD are the average of the triplicate of each test sample (n value of 1 \times 3). – value of No activity in disc diffusion assay Clotrim = Clotrimazole.

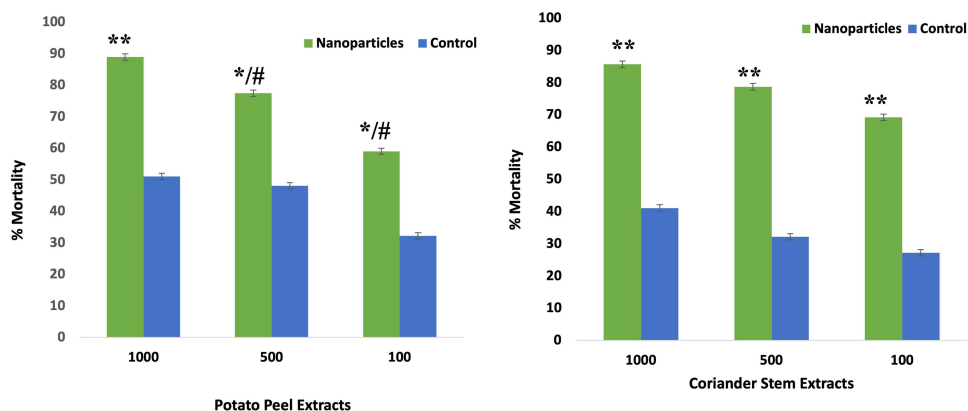


Figure 7 Comparative analysis of cytotoxic activity of AgNPs and crude extracts. Data are expressed as the mean \pm SD. */# $p < 0.05$, ** $p < 0.01$.

In contrast, the silver nanoparticles (AgNPs) synthesized from coriander also showed significant cytotoxic activity ie $85 \pm 0.32\%$ with an LC_{50} value of $31.62 \mu\text{g/mL}$ as compared to control extracts ie, $41 \pm 0.81\%$ with LC_{50} value of $94.57 \mu\text{g/mL}$ (Figure 7).

Cytotoxic Activity on HEp-2 Cell Lines

The cytotoxic activity of AgNPs from potato peel extracts on Hep-2 cell lines showed the highest activity with higher activity with 69% cell viability at the concentration of 20mg. Similarly, AgNPs from coriander stem extracts showed the highest activity with 67% viability of at the concentration of 20mg as compared to control extracts (100%) (Figure 8).

Antitumor Activity

The antitumor activity of both extracts was analyzed against the growth of *Agrobacterium tumefaciens*. The extracts derived from silver nanoparticles (AgNPs) showed significant activity in comparison with control extracts. AgNPs synthesized from potato peel extract showed significant tumor inhibition activity ie, $65 \pm 0.1\%$ with an IC_{50} value of $38.37 \mu\text{g/mL}$ as compared to control extracts ie, $30 \pm 0.18\%$ with an IC_{50} value of $182.56 \mu\text{g/mL}$ at the concentration of 1000 $\mu\text{g/mL}$ (Figure 9).

In contrast, the silver nanoparticles (AgNPs) synthesized from coriander showed the highest antitumor activity ie, $86 \pm 0.72\%$ with an IC_{50} value of $31.62 \mu\text{g/mL}$ as compared to control extracts ie, $21 \pm 0.92\%$ with IC_{50} value of $159.74 \mu\text{g/mL}$ at the concentration of 1000 $\mu\text{g/mL}$ (Figure 9).

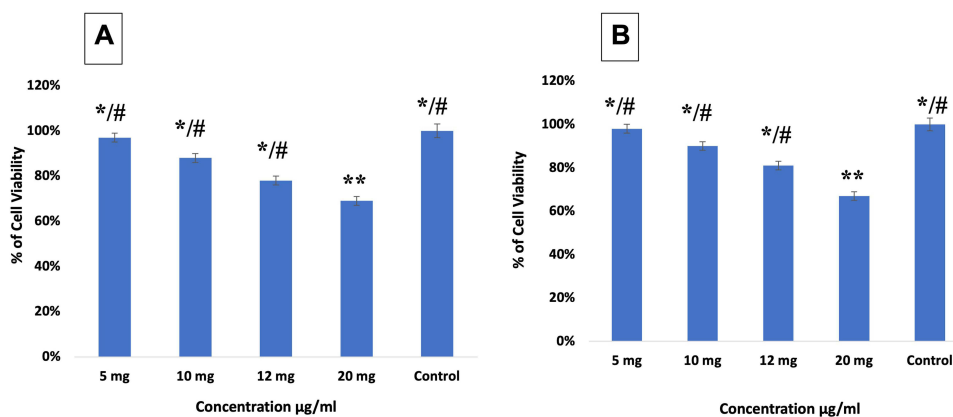


Figure 8 Comparative analysis of cytotoxicity activity of AgNPs and crude extracts on HEp2 Cell lines. Data are expressed as the mean \pm SD. */# $p < 0.05$, ** $p < 0.01$.

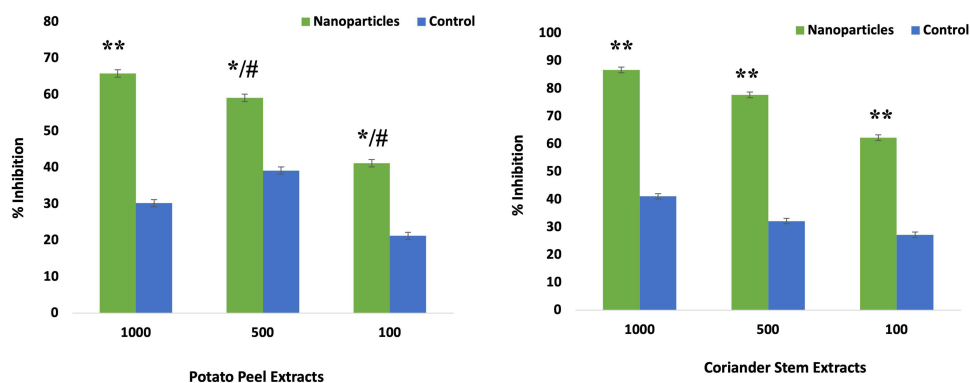


Figure 9 Comparative analysis of antitumor activity of AgNPs and crude extract. Data are expressed as the mean \pm SD. */# p < 0.05, ** p < 0.01.

Enzyme Inhibition Assays

Protein Kinase

Prominent clear and bald inhibition zones were observed in various crude extracts and AgNPs derived from those extracts. Notably, the AgNPs synthesized from coriander stem extract exhibited the largest bald zone of inhibition, measuring 49 mm. This indicates the potential antimicrobial activity of the coriander stem extract derived AgNPs. The AgNPs synthesized from potato peel extracts exhibited sufficient protein kinase inhibition activity. This result suggests that the AgNPs derived from these vegetable wastes have potent antimicrobial properties (Table 3).

α -Amylase Inhibition Assay

Both AgNPs derived from the extracts of vegetable waste demonstrated significant α -amylase inhibition activity. The AgNPs obtained from potato peel extracts interestingly exhibited the highest activity even more than positive control ($86.72 \pm 0.19\%$), with an inhibition rate of $96 \pm 0.19\%$, compared to the control with an inhibition rate of $53 \pm 0.7\%$.

These results indicate that the AgNPs derived from potato peel extracts possess strong α -amylase inhibitory potential. The AgNPs from the coriander stem extracts showed $85 \pm 0.98\%$ as compared to control ($65 \pm 0.21\%$) (Figure 10).

Discussion

Plants have consistently played a pivotal role in the field of medicine, serving as the primary source of naturally derived compounds, many of which have exhibited therapeutic effects. Many plants have medicinal properties such as anti-inflammatory, antitumor, antimicrobial, and antioxidant, making them valuable in the field of medicine. Different plants and their extracts contain different concentrations of essential compounds like phenol, flavonoids, antioxidant, and reducing agents. Recent studies showed the use of plants in the field of nanotechnology for a better, more effective, eco-friendly, less toxic method to synthesize metal nanoparticles.²⁰

Coriandrum sativum can easily grow globally and is used extensively as a medicinal plant. It also has nutritional values, and different parts of this plant reveal different properties. It contains many bioactive compounds which were

Table 3 Protein Kinase Inhibition Potential of Potato Peels, Coriander Stem and AgNPs

Plant Name	Samples	Numerical Value	Activity
Potato Peels	NP	11	Clear
	C	5	NA
Coriander Stems	NP	49	Bald
	C	5	NA

Notes: DMSO: negative control; Surfactin: positive control (20 μ g/disc; 16 mm zone).

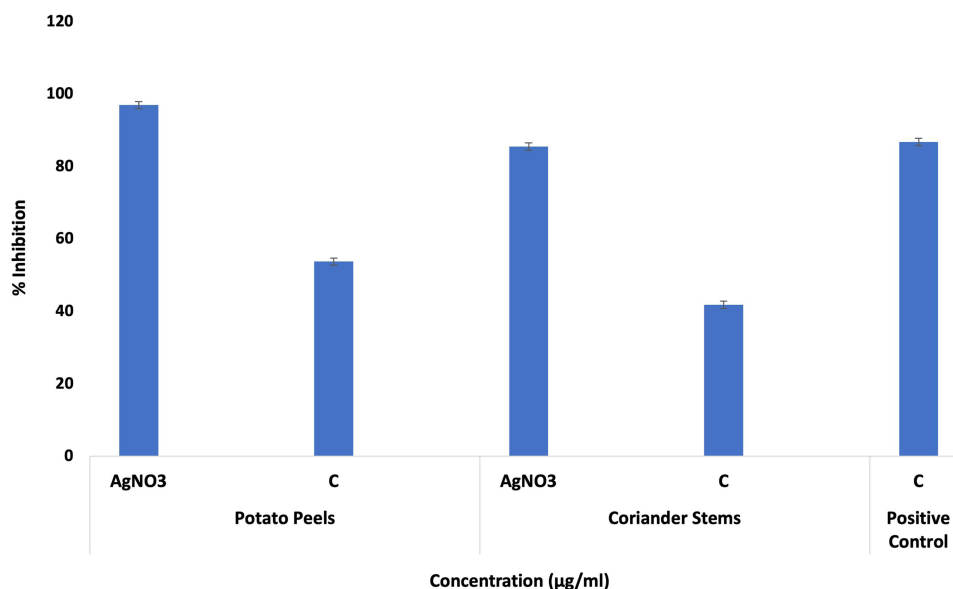


Figure 10 Comparison of α -amylase inhibition of various concentrations of AgNPs and crude extracts. Data are expressed as the mean \pm SD.

known to remove free radicals produced in cellular systems.²¹ *Solanum tuberosum* has also grown worldwide, is inexpensive and can easily be available whole year, and is widely consumed due to its appealing taste. It is known to decrease glycemic index due to its higher amylose/ amylopectin ratios.²²

Previous studies have provided evidence of significant silver nanoparticles (AgNPs) production using extracts derived from banana peels and tulsi leaves.^{23,24} These findings support the current study, where silver nanoparticles with remarkable size and shape were successfully synthesized. The objective of the present study was to synthesize silver nanoparticles using vegetable waste and to assess their medicinal bioactivities.

The vegetable waste extracts were prepared from potato peels, and coriander stems, and silver nitrate was added to the extracts for the synthesis of silver nanoparticles. The formation of synthesized nanomaterials was confirmed by a change in color from light yellow to brown. Further confirmation was obtained by UV spectroscopy, SEM analysis, and XRD. Sharma et al²⁵ reported that UV-Vis spectroscopy can be employed to analyze the shape and size of nanoparticles. UV spectroscopy has shown the peak of silver nanoparticles in the range of 300–400nm for both extracts (Figure 1A and B). SEM analysis showed a spherical and agglomerated shape with a particle size of 65nm for potato peels and 70nm for coriander stems (Figure 2A and B). XRD results have clearly shown the crystalline nature of silver nanoparticles. Peaks of XRD were at values of 20, 25, 30, 35, and 40 to 121, 200, 210, 220, and 311 planes (Figure 3A and B).

According to,²⁶ phytochemicals play a crucial role in treating various degenerative abnormalities. They have the capability of scavenging free radicals. They also inhibit the growth of microorganisms, inhibit lipid peroxidation, regulate gene expression, and have a crucial role in signal transduction pathways which make them very important medicinally.^{27–29} The results of the phytochemical assays demonstrated that the synthesis of AgNPs resulted in significant phenolic content in both potato peel and coriander stem extracts (Figure 4). In potato peel extracts, the AgNPs yielded a phenolic content of 58.23 ± 0.10 μ g GAE/mg, which was slightly lower than the control extracts (58.66 ± 0.81 μ g GAE/mg). Similarly, in coriander stem extracts, the AgNPs yielded a phenolic content of 58.66 ± 0.81 μ g GAE/mg, comparable to the control extracts. The flavonoid content also followed a similar pattern for both extracts (Figure 5). The AgNPs of potato peel extracts showed the highest flavonoid content, measuring 103.65 ± 0.76 μ g QE/mg. Meanwhile, the AgNPs of coriander stem extracts exhibited a flavonoid content of 105.62 ± 0.05 μ g QE/mg. These findings are in line with previous studies. Adebooye et al²⁹ reported a total phenol content of 0.704 mg GAE/g fresh weight in *S. nigrum* extracts, while³⁰ found a total phenol content of 180.64 ± 6.51 mg GAE/g in *C. tora* methanol extracts. Uddin et al³¹ reported a total phenol content of 3.6 ± 0.089 mg GAE/g in *P. oleracea* extracts. It is worth noting that slight variations in phenol content values can occur due to factors such as plant species, carotenoids, sugar content, duration, geographical variation, ascorbic acid, and

extraction methods. Overall, the synthesis of AgNPs from potato peels and coriander stems resulted in significant phenolic and flavonoid content, indicating their potential as sources of bioactive compounds.

In the current study, biological assays were conducted using silver nanoparticles synthesized from potato peel extract and coriander stem extract. The AgNPs derived from potato peels exhibited the highest scavenging activity with an IC_{50} value of 27.47 $\mu\text{g/mL}$, which was slightly lower than the control with an IC_{50} value of 28.57 $\mu\text{g/mL}$. The AgNPs from coriander stem extracts showed significant antioxidant activity with an IC_{50} of 27.47 as compared to the control with an IC_{50} of 28.57 $\mu\text{g/mL}$ (Figure 6). The crude extracts showed limited free radical scavenging potential at the tested concentrations. These findings align with previous studies conducted by,^{32–36} which also investigated nanoparticles derived from various plant species and reported similar results.

The green-synthesized AgNPs from vegetable waste extracts demonstrated significant antibacterial potential. AgNPs obtained from potato peel extracts exhibited the highest antibacterial activity against *E. coli*, with a zone of inhibition sizes measuring 20 ± 0.76 mm (MIC 100 $\mu\text{g/mL}$) and 23 ± 0.50 mm (MIC 33.3 $\mu\text{g/mL}$), respectively. AgNPs derived from coriander stem extracts displayed maximum antibacterial activity against *B. subtilis*, with a zone of inhibition measuring 18 ± 0.5 mm (MIC 100 $\mu\text{g/mL}$) (Table 1). These results suggest that the green synthesis of AgNPs from vegetable waste extracts enhances their antibacterial activity, highlighting their potential for further development as antimicrobial agents. This study aligns with the findings of,³⁷ which investigated the antimicrobial potential of plant extracts and found that nanoparticles exhibited higher activity compared to crude extracts.

The antifungal activity of test extracts showed the same pattern of activity, like antibacterial activity, where nanoparticles showed maximum activity in comparison with the control. The AgNPs derived from potato peel extracts exhibited the highest antifungal potential against *A. Flavus*, with a zone of inhibition measuring 15 ± 0.2 mm. On the other hand, the AgNPs from coriander stem extracts demonstrated maximum activity against *F. solani*, with a zone of inhibition measuring 11 ± 0.86 mm (Table 2). These results highlight the antimicrobial potential of the AgNPs extracts and suggest the need for further exploration and investigation of their potential clinical applications.³⁸ Proposed the Brine shrimp cytotoxicity assay as a suitable method for evaluating the pharmaceutical activities of plant extracts. The results of the cytotoxic assay conducted in this study indicated a significant effect in the crude extracts, while the AgNPs extracts were found to be even more effective. In the case of potato peel extracts, AgNPs showed maximum activity, ie, as compared to control extracts. Similar results were observed in coriander stem extracts where AgNPs showed an activity of 3.4% as compared to control extracts (Figure 7). The cytotoxicity of AgNPs is primarily associated with their large surface-to-volume ratio, which facilitates their entry into cells and interaction with cellular components. This interaction can disrupt cellular signaling pathways, contributing to their cytotoxic effects. It has been proposed that AgNPs can interact with mitochondria and interfere with the function of the cellular electron transfer chain, leading to an increase in the production of reactive oxygen species (ROS).³⁹

The antitumor potato disc assay is a valuable method for evaluating the antitumor activity of test compounds. In the current study, all the tested extracts demonstrated a high degree of inhibition of tumor formation (Figure 9). Notably, silver nanoparticles exhibited significant inhibition of tumour formation, with the potato peel extracts displaying the highest activity among the tested extracts. These findings highlight the potential of silver nanoparticles and vegetable waste extracts as promising candidates for further investigation and development for pharmaceutical purposes and to explore their potential applications in cancer treatment of different diseases. Furthermore, the cytotoxic activity of AgNPs and crude extracts were also analyzed on Hep-2 cell lines. The cytotoxic activity of AgNPs on Hep-2 cell lines showed higher activity with 67% viability of cells from coriander stem extracts at the concentration of 20mg. The AgNPs from potato peels showed 69% cell viability at the concentration of 20mg (Figure 8).

Diabetes mellitus is a metabolic syndrome characterized by high blood glucose levels. One strategy for managing blood glucose levels is inhibiting enzymes involved in carbohydrate hydrolysis, specifically α -amylase and α -glucosidase. Inhibiting these enzymes can slow down starch digestion and significantly control diabetes.⁴⁰ In the current study, AgNPs synthesized from potato peels and coriander stems exhibited superior inhibitory potential compared to the crude extracts. Among the AgNPs derived from potato peel extracts, the highest inhibitory activity of $47.67\pm 0.25\%$ was observed. Similarly, AgNPs from coriander stem extracts displayed maximum activity, with an inhibition rate of $38.01\pm 0.78\%$ (Figure 10). These findings highlight the promising inhibitory potential of AgNPs extracts against α -amylase and

α -glucosidase, suggesting their potential for managing diabetes. Further research is required to explore their mechanisms of action and potential clinical applications in diabetes management.

Protein kinases play a crucial role in oncogenesis, as uncontrolled phosphorylation due to these kinases can lead to the development of cancer by altering genetic signaling.⁴¹ Therefore, it is important to investigate herbal products with cytotoxic potential for their ability to inhibit protein kinase activity. In the present study, the AgNPs derived from potato peel extracts demonstrated the maximum bald zone of inhibition, measuring 12 mm, indicating their potential as inhibitors of hyphae formation.¹⁵ On the other hand, the AgNPs derived from coriander stem extracts resulted in a bald zone of inhibition measuring 8 mm (Table 3). These results suggest that the AgNPs extracts, particularly those from potato peel, can inhibit protein kinases, leading to the inhibition of hyphae formation in *Streptomyces*. Further research is needed to explore the specific mechanisms of action and potential applications of these extracts in controlling protein kinase activity and its associated effects.

Conclusion

The present study introduces a simple and effective method for synthesizing silver nanoparticles using extracts prepared from vegetable waste. One of the key advantages of this synthesis method is its efficiency, cost-effectiveness, sustainability and environmentally friendly nature. Silver nanoparticles with small size and shape were successfully synthesized from peels of potato and stems of coriander at a persistent rate. The silver nanoparticles were crystalline in nature, spherical, and agglomerated in shape, with sizes of 65 and 70 nm. Silver nanoparticles exhibited significant antimicrobial activity, cytotoxic activity, antioxidant activity, antitumor activity, tumor inhibition activity against HEP2 cell lines and enzyme inhibition properties. These green synthesized silver nanoparticles lead to low-budget, safe, and nonhazardous alternatives to physical, chemical as well as microbiological methods and would be appropriate for wide-scale production. The multi-pharmacological properties of these nanoparticles make them promising candidates for treating various diseases and use of vegetable waste extracts as a raw material for nanoparticle synthesis aligns with the increasing demand from drug manufacturers for sustainable and eco-friendly alternatives. Overall, this study opens new possibilities for utilizing vegetable waste extracts in nanoparticle synthesis and highlights the potential of these nanoparticles in various therapeutic applications. The efficient and environmentally friendly nature of this synthesis method makes it a promising approach for meeting the growing demand for multifunctional nanoparticles in the field of medicine.

Ethics Approval

The present study followed national guidelines of Pakistan National Bioethics Committee for Research for animal treatment. The Pakistan National Bioethics committee and Institutional Review Board and Ethics Committee of International Islamic University, Islamabad reviewed and approved this study under relevant legislation from Pakistan's Prevention of Cruelty to Animals Act 1890.

No additional approvals were required to conduct research with plant material, in accordance with institutional/local regulations.

Acknowledgment

The authors extend their appreciation to the Researchers Supporting Project number (RSPD2023R725) King Saud University, Riyadh, Saudi Arabia.

Author Contributions

All authors made a significant contribution to the work reported, whether that is in the conception, study design, execution, acquisition of data, analysis and interpretation, or in all these areas; took part in drafting, revising or critically reviewing the article; gave final approval of the version to be published; have agreed on the journal to which the article has been submitted; and agree to be accountable for all aspects of the work.

Funding

The funding for this project was provided by the Researchers Supporting Project number (RSPD2023R725) King Saud University, Riyadh, Saudi Arabia.

Disclosure

The authors report no conflicts of interest in this work.

References

1. Silva GA. Nanotechnology approaches for the regeneration and neuroprotection of the central nervous system. *Surg Neurol.* 2005;63(4):301–306. doi:10.1016/j.surneu.2004.06.008
2. Ahmad P, Mukherjee A, Mandal D, et al. Fungus-mediated synthesis of silver nanoparticles and their immobilization in the mycelial matrix: a novel biological approach to nanoparticle synthesis. *Nano Lett.* 2001;1(10):515–519. doi:10.1021/nl0155274
3. Oves M, Rauf MA, Qari HA. Therapeutic applications of biogenic silver nanomaterial synthesized from the paper flower of bougainvillea glabra (Miami, pink). *Nanomaterials.* 2023;13(3):615. doi:10.3390/nano13030615
4. Oves M, Ahmar Rauf M, Aslam M. Green synthesis of silver nanoparticles by Conocarpus Lancifolius plant extract and their antimicrobial and anticancer activities. *Saudi J Biol Sci.* 2022;29(1):460–471. doi:10.1016/j.sjbs.2021.09.007
5. Henriquez C, Speisky H, Chiffelle I, et al. Development of an ingredient containing apple peel, as a source of polyphenols and dietary fiber. *J Food Sci.* 2010;75(6):H172–H181. doi:10.1111/j.1750-3841.2010.01700.x
6. Savitri D, Djawad K, Hatta M, Wahyuni S, Bukhari A. Active compounds in kepek banana peel as anti-inflammatory in acne vulgaris. *Ann Med Surg.* 2022;12:104868.
7. Sampaio SL, Petropoulos SA, Alexopoulos A, et al. Potato peels as sources of functional compounds for the food industry: a review. *Trends Food Sci Technol.* 2020;103:118–129. doi:10.1016/j.tifs.2020.07.015
8. Zahoor M, Nazir N, Iftikhar M, et al. A review on silver nanoparticles: classification, various methods of synthesis, and their potential roles in biomedical applications and water treatment. *Water.* 2021;13(16):2216. doi:10.3390/w13162216
9. Wang L, Hu C, Shao L. The antimicrobial activity of nanoparticles: present situation and prospects for the future. *Int J Nanomedicine.* 2017;14:1227–1249. doi:10.2147/IJN.S121956
10. Shankar SS, Rai A, Ahmad A, Sastry M. Controlling the optical properties of lemongrass extract synthesized gold nanotriangles and potential application in infrared-absorbing optical coatings. *Chemist Mater.* 2005;17(3):566–572. doi:10.1021/cm048292g
11. Pal S, Tak YK, Song JM. Does the antibacterial activity of silver nanoparticles depend on the shape of the nanoparticle? A study of the gram-negative bacterium Escherichia coli. *Appl Environ Microbiol.* 2007;73(6):1712–1720. doi:10.1128/AEM.02218-06
12. Mayerhöfer TG, Pahlow S, Popp J. The Bouguer-Beer-Lambert law: shining light on the obscure. *Chem Phys Chem.* 2020;21(18):2029–2046. doi:10.1002/cphc.202000464
13. Schaffer M, Schaffer B, Ramasse Q. Sample preparation for atomic-resolution STEM at low voltages by FIB. *Ultramicroscopy.* 2012;114:62–71. doi:10.1016/j.ultramic.2012.01.005
14. Nasar MQ, Zohra T, Khalil AT, et al. Extraction optimization, Total Phenolic-Flavonoids content, HPLC-DAD finger printing, antimicrobial, antioxidant and cytotoxic potentials of Chinese folklore Ephedra intermedia Schrenk & CA Mey. *Braz J Pharm Sci.* 2023;58. doi:10.1590/s2175-97902022e20989
15. Zahra SS, Ahmed M, Qasim M, et al. Polarity based characterization of biologically active extracts of Ajuga bracteosa Wall. Ex Benth. and RP-HPLC analysis. *BMC Complement Altern Med.* 2017;17(1):1–6. doi:10.1186/s12906-017-1951-5
16. Satyavani K, Gurudeeban S, Ramanathan T, Balasubramanian T. Toxicity study of silver nanoparticles synthesized from Suaeda monoica on Hep-2 cell line. *Avicenna J Med Biotechnol.* 2012;4(1):35.
17. Adebisi OE, Olayemi FO, Ning-Hua T, Guang-Zhi Z. In vitro antioxidant activity, total phenolic and flavonoid contents of ethanol extract of stem and leaf of Grewia carpinifolia. *Beni Suef Univ J Basic Appl Sci.* 2017;6(1):10–14. doi:10.1016/j.bjbas.2016.12.003
18. Tariq H, Zia M, Khan SA, et al. Antioxidant, antimicrobial, cytotoxic, and protein kinase inhibition potential in Aloe vera L. *Biomed Res Int.* 2019;2019:1–14. doi:10.1155/2019/6478187
19. Magaji UF, Sacan O, Yanardag R. Alpha amylase, alpha glucosidase and glycation inhibitory activity of Moringa oleifera extracts. *South Afr J Botany.* 2020;128:225–230. doi:10.1016/j.sajb.2019.11.024
20. Alviano DS, Alviano CS. Plant extracts: search for new alternatives to treat microbial diseases. *Curr Pharm Biotechnol.* 2009;10(1):106–121. doi:10.2174/138920109787048607
21. Mahleyuddin NN, Moshawih S, Ming LC, et al. Coriandrum sativum L.: a review on ethnopharmacology, phytochemistry, and cardiovascular benefits. *Molecules.* 2021;27(1):209. doi:10.3390/molecules27010209
22. Reddivari L, Wang T, Wu B, Li S. Potato: an anti-inflammatory food. *Am J Potato Res.* 2019;96(2):164–169. doi:10.1007/s12230-018-09699-z
23. Ibrahim HM. Green synthesis and characterization of silver nanoparticles using banana peel extract and their antimicrobial activity against representative microorganisms. *J Radiat Res Appl Sci.* 2015;8(3):265–275. doi:10.1016/j.jrras.2015.01.007
24. Tailor G, Yadav BL, Chaudhary J, Joshi M, Suvalka C. Green synthesis of silver nanoparticles using Ocimum canum and their anti-bacterial activity. *Biochem Biophys Rep.* 2020;24:100848. doi:10.1016/j.bbrep.2020.100848
25. Sharma NK, Vishwakarma J, Rai S, Alomar TS, AIMasoud N, Bhattarai A. Green route synthesis and characterization techniques of silver nanoparticles and their biological adeptness. *ACS omega.* 2022;7(31):27004–27020. doi:10.1021/acsomega.2c01400
26. Forni C, Faechiano F, Bartoli M, et al. Beneficial role of phytochemicals on oxidative stress and age-related diseases. *Biomed Res Int.* 2019;2019:1–16. doi:10.1155/2019/8748253
27. George BP, Chandran R, Abrahamse H. Role of phytochemicals in cancer chemoprevention: insights. *Antioxidants.* 2021;10(9):1455. doi:10.3390/antiox10091455

28. Sumbul S, Ahmad MA, Mohd A, Mohd A. Role of phenolic compounds in peptic ulcer: an overview. *J Pharm Bioallied Sci.* 2011;3(3):361. doi:10.4103/0975-7406.84437
29. Adebooye OC, Vijayalakshmi R, Singh V. Peroxidase activity, chlorophylls and antioxidant profile of two leaf vegetables (*Solanum nigrum* L. and *Amaranthus cruentus* L.) under six pretreatment methods before cooking. *Int J Food Sci Technol.* 2008;43(1):173–178. doi:10.1111/j.1365-2621.2006.01420.x
30. Yen GC, Chuang DY. Antioxidant properties of water extracts from *Cassia tora* L. in relation to the degree of roasting. *J Agric Food Chem.* 2000;48(7):2760–2765. doi:10.1021/jf991010q
31. Uddin MK, Juraimi AS, Ali ME, Ismail MR. Evaluation of antioxidant properties and mineral composition of purslane (*Portulaca oleracea* L.) at different growth stages. *Int J Mol Sci.* 2012;13(8):10257–10267. doi:10.3390/ijms130810257
32. Parry J, Su L, Luther M, et al. Fatty acid composition and antioxidant properties of cold-pressed marionberry, boysenberry, red raspberry, and blueberry seed oils. *J Agric Food Chem.* 2005;53(3):566–573. doi:10.1021/jf048615t
33. Prior RL, Wu X, Schaich K. Standardized methods for the determination of antioxidant capacity and phenolics in foods and dietary supplements. *J Agric Food Chem.* 2005;53(10):4290–4302. doi:10.1021/jf0502698
34. Zhou K, Yin JJ, Yu L. Phenolic acid, tocopherol and carotenoid compositions, and antioxidant functions of hard red winter wheat bran. *J Agric Food Chem.* 2005;53(10):3916–3922. doi:10.1021/jf050117c
35. Sadighara P, Moghadam Jafari A, Khaniki GJ, Shariati N, Lotfi AA. Potential therapeutic effects of *Morus alba* leaf extract on modulation oxidative damages induced by hyperglycemia in cultured fetus fibroblast cells. *Global Veterinaria.* 2013;10:35–38.
36. Ghagane SC, Puranik SI, Kumbhar VM, et al. In vitro antioxidant and anticancer activity of *Leea indica* leaf extracts on human prostate cancer cell lines. *Integrat Med Res.* 2017;6(1):79–87. doi:10.1016/j.imr.2017.01.004
37. Dildar A, Saeed R, Shakeel N, Fatima K, Arshad A. Antimicrobial activities of methanolic extract of *Carissa opaca* roots and its fractions and compounds isolated from the most active ethyl acetate fraction. *Asian Pac J Trop Biomed.* 2015;5(7):541–545. doi:10.1016/j.apjtb.2015.05.006
38. Carballo JL, Hernández-Inda ZL, Pérez P, García-Grávalos MD. A comparison between two brine shrimp assays to detect in vitro cytotoxicity in marine natural products. *BMC Biotechnol.* 2002;2(1):1–5. doi:10.1186/1472-6750-2-17
39. Bressan E, Ferroni L, Gardin C, et al. Silver nanoparticles and mitochondrial interaction. *Int J Dent.* 2013;2013:1–8. doi:10.1155/2013/312747
40. Poovitha S, Parani M. In vitro and in vivo α -amylase and α -glucosidase inhibiting activities of the protein extracts from two varieties of bitter melon (*Momordica charantia* L.). *BMC Complement Altern Med.* 2016;16(1):1–8. doi:10.1186/s12906-016-1085-1
41. Vizeacoumar FS, Vizeacoumar FJ, Freywald A, Giambra V, Freywald A, Giambra V. Protein tyrosine kinases: their roles and their targeting in leukemia. *Cancers.* 2021;13(2):184. doi:10.3390/cancers13020184

International Journal of Nanomedicine

Dovepress

Publish your work in this journal

The International Journal of Nanomedicine is an international, peer-reviewed journal focusing on the application of nanotechnology in diagnostics, therapeutics, and drug delivery systems throughout the biomedical field. This journal is indexed on PubMed Central, MedLine, CAS, SciSearch®, Current Contents®/Clinical Medicine, Journal Citation Reports/Science Edition, EMBASE, Scopus and the Elsevier Bibliographic databases. The manuscript management system is completely online and includes a very quick and fair peer-review system, which is all easy to use. Visit <http://www.dovepress.com/testimonials.php> to read real quotes from published authors.

Submit your manuscript here: <https://www.dovepress.com/international-journal-of-nanomedicine-journal>